Journal of Applied Physics

RESEARCH ARTICLE | SEPTEMBER 03 2025

A first-principles investigation of halogen doped diamond and its application to quantum technologies

Petros-Panagis Filippatos ; Alexander Chroneos ; Nikolaos Kelaidis

Check for updates

J. Appl. Phys. 138, 094401 (2025)
https://doi.org/10.1063/5.0279139

View Online Export Citation

Articles You May Be Interested In

Ab initio investigation of the Cr substitutional defect in α-quartz for quantum applications

J. Appl. Phys. (December 2025)

Hydrogen bond and halogen bond inside the carbon nanotube

J. Chem. Phys. (February 2011)

On the ultrafast charge migration and subsequent charge directed reactivity in Cl···N halogen-bonded clusters following vertical ionization

J. Chem. Phys. (June 2015)

31 July 2026 06:30:23

AIP Publishing

Journal of Applied Physics ARTICLE pubs.aip.org/aip/jap

A first-principles investigation of halogen doped diamond and its application to quantum technologies

Cite as: J. Appl. Phys. **138**, 094401 (2025); doi: 10.1063/5.0279139
Submitted: 6 May 2025 · Accepted: 12 August 2025 ·
Published Online: 3 September 2025

View Online Export Citation CrossMark

Petros-Panagis Filippatos,[1,a)] Alexander Chroneos,[2,3] and Nikolaos Kelaidis[4]

AFFILIATIONS

[1]School of Chemistry, University of Nottingham, Nottingham NG7 2RD, United Kingdom
[2]Department of Electrical and Computer Engineering, University of Thessaly, 38221 Volos, Greece
[3]Department of Materials, Imperial College London, London SW7 2AZ, United Kingdom
[4]National Hellenic Research Foundation, Theoretical and Physical Chemistry Institute, Vass. Constantinou 48, GR-11635 Athens, Greece

[a)]**Author to whom correspondence should be addressed:** pczpf@exmail.nottingham.ac.uk

ABSTRACT

Defect centers in diamond have attracted considerable attention for the development of emerging quantum technologies, for example, quantum sensors and spin qubits. Nitrogen vacancy (NV) is the most well-studied and utilized defect; however, its relatively high zero phonon line (ZPL) is responsible for optical losses and limiting efficiency. Here, we focus on the halogen doping in diamond, employing the strongly constrained and appropriately normed meta-generalized gradient approximation functional to investigate the thermodynamic and electronic properties of these defects. We analyzed all stable charge states at their lowest energy spin state and identified qubit candidates with paramagnetic ground states and optically addressable transitions, suitable for quantum applications. We focus on the fluorine substitutional defect at negative charge (F_C^{-1}), which we found as a promising spin-defect that has not been extensively investigated before. We predict that it has a triplet ground state and a ZPL much lower compared to the NV center that falls into the desired telecommunication range. To describe its qubit operation protocol, we calculate the zero-field splitting and the hyperfine tensors. The present findings suggest that F_c has very promising properties and could be a viable alternative to traditional qubits in diamond.

© 2025 Author(s). All article content, except where otherwise noted, is licensed under a Creative Commons Attribution (CC BY) license (https://creativecommons.org/licenses/by/4.0/). https://doi.org/10.1063/5.0279139

31 July 2026 06:30:23

I. INTRODUCTION

In essence, quantum technologies rely on encoded quantum bits (qubits) that enable applications in computing, communication, and sensing. In that respect, spin dependent color centers in semiconductors are promising candidates for solid-state qubits.[1–3] Defect centers can operate as single-photon sources or spin-photon interfaces possessing a spin degree of freedom. This, in turn, can enable the generation and distribution of entangled photons in quantum networks and is important for quantum information science.[4,5] To be plausible as qubits, defects need to have strong transition dipole moments, long spin coherence times, minimal losses in the phonon sideband of photoluminescence, high optical coherence, and a suitable zero phonon line (ZPL) in the telecom range.[6]

The archetypal defect in diamond is the nitrogen-vacancy (N*V*) center as it is an extensively investigated spin defect for quantum applications.[7–9] The N*V* center allows optical initialization, readout, and coherent spin manipulation, and this constitutes it a good candidate for spin-based quantum technologies and has been experimentally demonstrated as a qubit.[7–11] However, the reliance on defect centers as qubits is plagued by the uncontrolled defect diffusion and formation during fabrication given that chemical vapor deposition (CVD) and high-energy ion implantation cannot accurately control defects.[12,13] Over the years, many other structures have been proposed for quantum technologies and, in the recent years, 2D materials have also been examined as alternative hosts to diamond due to the low dimensional nuclear spin

© Author(s) 2025

baths, absence of dangling bonds at the surface, and compatibility with advanced fabrication techniques for large scale production.[14–16] Regardless of the above-mentioned drawbacks, diamond is still being investigated theoretically and experimentally with alternative defect strategies. Thiering and Gali[17] investigated the substitutional nickel defect (Ni_s) in diamond, a defect that exhibits Td symmetry and paramagnetic ground state at the neutral charge. In this work, the authors analyzed the effect of spin–orbit coupling (SOC) and Jahn–Teller effects and investigated the optical transitions coming from the transition metal. In another recent paper, Davidsson *et al.*[18] presented a high-throughput screening of point defects in diamond and identified sodium-related defects as especially promising for quantum applications due to their high-spin states, near infrared ZPLs, and strong Debye–Waller factors. A related Na–V center defect hosts a rare spin-2 ground state, which could also be used for encoding quantum information. As such, the examination of alternative defects and their extensive theoretical investigation is crucial.

Halogen doping in group IV elements has been investigated in the community as a way to control diffusion and enhance electrical activation. In particular, fluorine (F) doping retards *n*-type dopant diffusion and increases the donor electrical activation in highly doped *n*-type doped germanium (Ge).[19,20] In silicon (Si) and silicon germanium ($Si_{1-x}Ge_x$), F reduces the transient enhanced diffusion (TED) of boron (B) while enhancing its electrical activation.[21,22] Considering diamond, halogen dopants have been previously studied in the bulk and surface, aiming to improve its electrical and optical properties.[23–31] For example, in the DFT study by Yan *et al.*,[23] the electronic properties of diamond doped with halogen (F, Cl, Br, and I) atoms were considered and concluded that F acts as an acceptor, but Cl, Br, and I constitute donor behavior. Ditalia Tchernij *et al.*[31]experimentally investigated F based color centers in diamond and determined optical activity from the F-vacancy defect highlighting their potential importance for quantum sensing and quantum computation. While this study was very interesting, an extensive theoretical investigation of the potential of F or other halogens has not still been performed.

In a previous work, Weber *et al.*[32] proposed a set of rules for the ideal quantum defect host and these are commonly applied for DFT investigations of defect based qubits. Specifically, in this work, the authors postulated that the host crystal should have a wide bandgap, small spin–orbit coupling strength, paramagnetic accessible states, and at least two bound states, which are separated from each other, in order to avoid thermal excitation. However, there are also proposed quantum host systems that have been investigated that do not obey all these rules.[33–36] The room-temperature (295 K) operation of defect-based qubits and single-photon emitters also requires the emitter to have charge-state stability (i.e., both the ground and excited states should be sufficiently deep within the bandgap avoiding electron exchange with the host's bulk bands). Spin-state stability is important to avoid non-emissive dark states caused by uncontrolled spin dynamics, and therefore small spin–orbit coupling (SOC) is required.[32] Paramagnetic states facilitate the magnetic resonance-based spin control and readout, and the robust initialization protocols through optical or spin-selective transitions in solid-state defect qubits.[37] Importantly, spin sublevels can be individually addressed and manipulated and this is the key for quantum sensing, memory, and entanglement protocols. The determining parameter is the zero-field splitting (ZFS) that lifts the degeneracy of spin sublevels even without an external magnetic field, and this enables coherent spin manipulation at fixed microwave frequencies.[37] Furthermore, the hyperfine interaction couples the electron spin to nearby nuclear spins and this provides a way for long-lived quantum memory and multi-qubit registers.[38] The ZFS and hyperfine constants define the spin Hamiltonian governing the fidelity and resolution of spin initialization, control, and readout.

Based on recent advances in both experimental and theoretical observations, this work focuses on the extensive simulation of halogen substitutionals in diamond, which we demonstrate to be promising candidates for scalable quantum technologies. We calculate the formation energies along with the electronic and magnetic properties. We find that the introduction of F_C and paramagnetic ground state enables efficient spin-photon interfaces suitable for quantum applications, and we also calculate the radiation lifetime for the spin allowed transition. Furthermore, we find an accessible low-spin singlet state which is located between the ground and the excited triplet, enabling the intersystem crossing pathway similar to the NV-center in diamond. Finally, for F_C, we calculate the ZFS and the hyperfine interaction, and we discuss the potential qubit operation protocol.

II. METHODOLOGY

A. Computational details

The DFT calculations were performed using the Vienna *Ab initio* Simulation Package (VASP).[39–41] All calculations were performed using spin polarized DFT with the projector augmented wave (PAW) pseudopotentials.[41,42] In our calculations, the explicitly treated valence electrons for carbon were $2s^2\ 2p^2$, and for halogens (F, Cl, Br, and I), the explicitly treated valence electrons were $2s^2\ 2p^5$ (F), $3s^2\ 3p^5$ (Cl), $4s^2\ 4p^5$ (Br), and $5s^2\ 5p^5$ (I), respectively, as described by the PAW pseudopotentials. We employed the strongly constrained and appropriately normed (SCAN) meta-generalized gradient approximation (meta-GGA) functional.[43] The plane wave cutoff energy was 850 eV in conjunction with a $4 \times 4 \times 4$ k-point set. Total energies converged using the rule of 1 meV/atom for the self-consistent field (SCF) loop while the residual forces were less than 0.01 eV/Å. To negate the interaction of the defect with its image due to periodic boundary conditions, we used a supercell consisting of 216 atoms with 10.66 Å in each direction. For the identification of the correct ground state of the defect structures, we employed the ShakeNBreak method. The efficacy of the present methodology has been demonstrated in previous studies on related issues on a number of systems.[43,44]

B. Defect calculations

The formation energy of the halogen dopant in diamond defects is defined as the energy difference between the doped system and the components in their reference state. For a defect *D* at a charge state *q*, the formation energy is defined as

$$\Delta H_{D,q}(E_f, \mu) = [E_{D,q} - E_H] - \sum n_i \mu_i + qE_f + E_{\text{corr}}, \quad (1)$$

31 July 2026 06:30:23

© Author(s) 2025

where $E_{D,q}$ is the total energy of the supercell containing defect D at charge state q and E_H is the energy of the defect-free supercell of diamond. n_i is the number of atoms of type i that are added ($n_i > 0$) or removed ($n_i < 0$) with chemical potentials μ_i, and E_f is the Fermi level relative to the valence band maximum (VBM) eigenvalue energy (serves as a free parameter). E_{corr} is the term that includes the charge image and potential alignment corrections.[45]

The chemical potentials μ_i are variables, which account for the experimental synthesis conditions. In this work, μ_C is referenced to the total energy of a single C atom in the bulk diamond crystal, while the chemical potentials of halogens are calculated with respect to the gas molecules. Specifically, we used a wide box of 10 Å and placed the gas molecules in the center. After performing geometry optimization, we found the energy of the molecule and then divided the energy by the number of atoms to find the chemical potential of the atom. The calculation of chemical potentials was done following the doped software workflow.[46]

The defect charge transition levels (CTLs) between two charges q and q' are computed using the formation energies as follows:

$$\varepsilon(q/q') = \frac{E^f(\mathrm{D}, \mathrm{q}; E_F = 0) - E^f(\mathrm{D}, \mathrm{q}'; E_F = 0)}{q' - q}, \tag{2}$$

where $E^f(\mathrm{D}, \mathrm{q}; E_F = 0)$ and $E^f(\mathrm{D}, \mathrm{q}'; E_F = 0)$ represent the formation energies of the defect in charge states q and q', respectively, evaluated at the VBM (i.e., for $E_F = 0$). To determine these levels, formation energies of the defects at different charge states were calculated, and the CTLs were identified as the values of the Fermi level at which two different charged defect states have equal formation energies.

C. Optical excitations and radiation lifetime

To investigate the electronic and optical excitations, we performed constrained Density Functional Theory (cDFT), also called the Delta-SCF (Δ-SCF) approach. This method enables control over the occupation of defect localized electronic states, facilitating the simulation of the excited state geometry. In cDFT, the excited state energy of a point defect is obtained by promoting an electron from the last occupied level to the first unoccupied, within the bandgap. The new occupation of the selected orbitals is kept fixed during the self-consistent Kohn–Sham calculations, while allowing the atomic structure to relax. The energy difference between the ground state and the relaxed excited state represents the ZPL energy. This method has shown great results compared to experiments for various qubit hosts, such as NV centers[9] in diamond and V_B^{-1} in hBN.[47]

After calculating the ZPL, we can calculate the radiation lifetime of the spin allowed excitation. The radiation lifetime can be estimated using the Wigner–Weisskopf theory, utilizing the wavefunction of the ground state and the wavefunction of the relaxed excited state. To process the wavefunction data, we used a modified version of the PyVaspwfc code.[48] The excitation lifetime was then estimated as[49]

$$\frac{1}{\tau} = \frac{n_r (2\pi)^3 \nu^3 |\mu|^2}{3\varepsilon_0 h c^3}, \tag{3}$$

where τ is the excitation lifetime, n_r is the refractive index, and ϵ_0 is the vacuum permittivity. h and c represent the Planck constant and the speed of light in a vacuum, respectively. μ represents the transition dipole moment, which is calculated as

$$\mu_k = \frac{i\hbar}{(\epsilon_{f,k} - \epsilon_{i,k})m} \left\langle \psi_{f,k} | p | \psi_{i,k} \right\rangle, \tag{4}$$

where $\epsilon_{i,k}$and $\epsilon_{f,k}$ represent the eigenvalues of the initial and final states, m is the electron mass, $\psi_{i,k}$ and $\psi_{f,k}$ are the initial and final wavefunctions, and p is the momentum operator.

D. Zero-field splitting and hyperfine tensors

We further calculate the ZFS parameters for potential halogen qubit candidates with triplet ground states, using *ab initio* calculations. ZFS refers to the energy separation between the magnetic sublevels in systems with paramagnetic spin, caused by the spin–orbit or spin–spin interaction. For halogen doped diamond, the spin–orbit interactions are negligible and, as a result, we present the values for dipolar spin–spin only. The contributions were calculated as discussed in Refs. 50–52 yielding the axial (D) and rhombic (E) components that define the total ZFS tensor. The ZFS is a very important parameter of the operation of quantum sensors using the optically detected magnetic resonance (ODMR) technique.[53]

The hyperfine tensor represents the interaction between an electron spin S and a nuclear spin J and is given by

$$A_{ij} = \frac{1}{2S} \gamma_J \gamma_e \hbar^2 \left[\frac{8\pi}{3} \int \delta(r - R_J) \sigma(r) dr + W_{ij}(R_J) \right], \tag{5}$$

where the first term in the square brackets represents the Fermi-contact isotropic term and

$$W_{ij}(R) = \int \left(\frac{3(r-R)_i (r-R)_j}{|r-R|^5} - \frac{\delta_{ij}}{|r-R|^3} \right) \sigma(r) dr \tag{6}$$

is the dipole–dipole anistotropic contribution. γ_J, γ_e is the nuclear magneton of nucleus J and the electron Bohr magneton, respectively, while $\sigma(r)$ describes the electron spin density. After diagonalization, the three main values are labeled as A_{xx}, A_{yy}, and A_{zz}. The calculations of the hyperfine interaction and the Fermi contact are implemented in VASP.[54]

III. RESULTS AND DISCUSSION

A. Thermodynamical properties

Bulk diamond has a cubic structure and belongs to the Fd3m space group.[55] Using SCAN, we calculated the optimized lattice parameters at a = b = c = 3.55 Å, which is in good agreement with the experimental values of 3.57 Å.[56] The bandgap value is

31 July 2026 06:30:23

© Author(s) 2025

calculated at 4.54 eV, which is underestimated compared to the experimental value of 5.5 eV, but improved compared to the local density approximation (LDA) or PBE calculations (4.2 eV).[9] As it was shown in previous studies,[44,57] while meta-GGA tends to underestimate the bandgap, this does not affect the calculation of the zero phonon line; thus, it is a good alternative to the highly computationally cost HSE06 functional.

To identify the stable charge states of the halogen defects, we use the formation energy diagrams and their calculation is explained in the methodology section. For these diagrams, we identify the correct spin multiplicity of the defect that represents the correct ground state. This investigation is very crucial because the paramagnetic ground states are the ones to encode quantum information. Figures 1(a)–1(d) display the formation energies for substitutional halogen defects in diamond, calculated using the SCAN functional. The equation for plotting these graphs is discussed in the methodology section. We tested the formation energies for charges ranging from −2 to 2 as a function of the Fermi level, and for all halogens, we found that −1, 0, and +1 are stable. The vertical spans of the Fermi level range from the valence band maximum to the conduction band minimum. As we can see from Fig. 1, F_C^0 has the lowest formation energy equal to 6.49 eV, while the transition ε (+1/0) is happening at 0.64 eV and ε(0/−1) at 3.10 eV. As we move to the substitution with heavier elements, such as Cl, Br, and I, the formation energy of the neutral charge increases. For instance, Cl_C^0 exhibits overall high formation energy equal to 14.83 eV, while Br_c^0 and I_c^0 have formation energies of 18.78 and 24.58 eV, respectively. These extremely high formation energies across all halogen substitutes indicate that under thermodynamic equilibrium, halogen substitutional defects are unlikely to form in significant concentrations in bulk diamond. Thus, intentional doping with non-equilibrium techniques such as ion implantation or plasma-enhanced growth methods will be necessary to introduce and stabilize these quantum related centers.

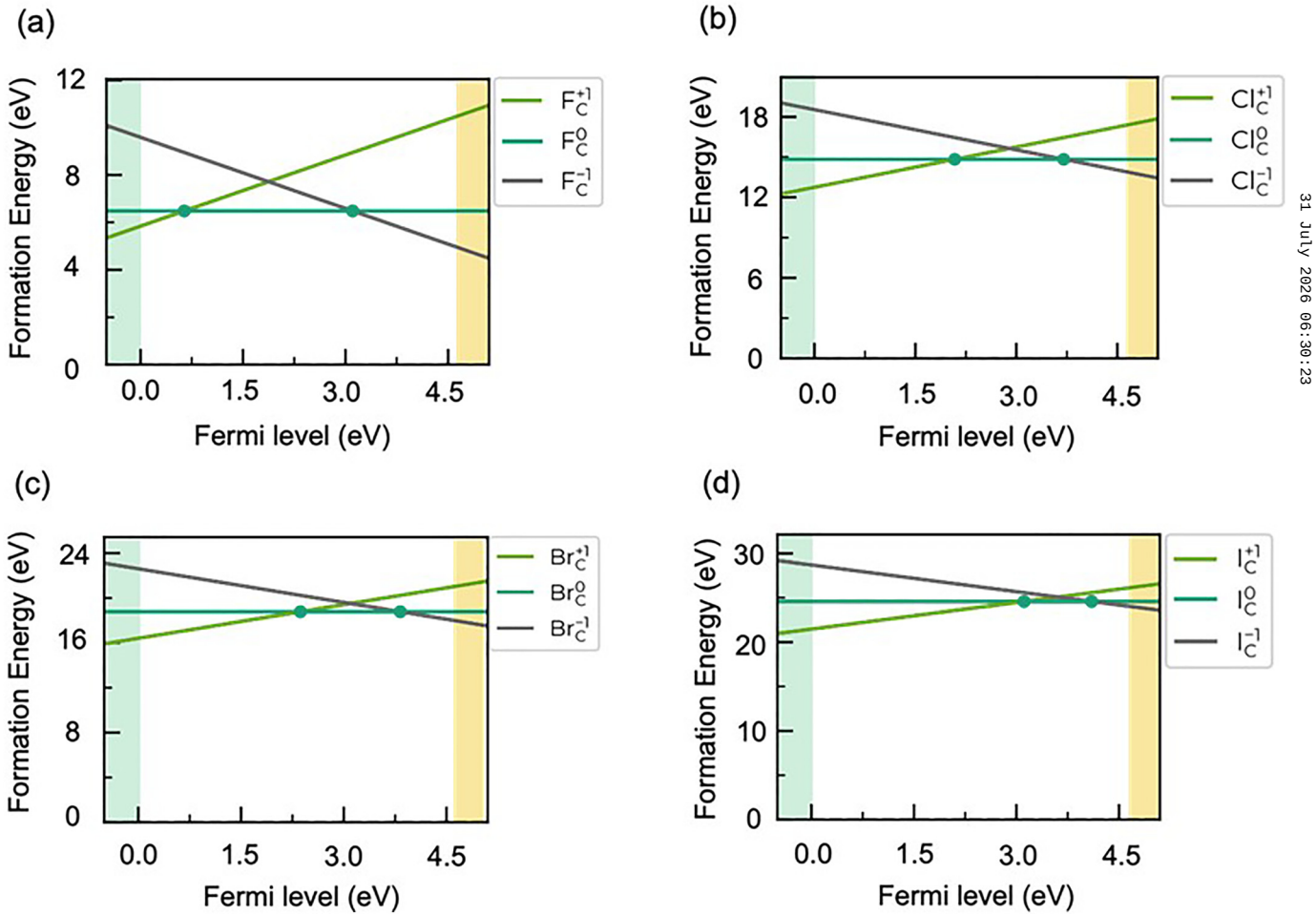

FIG. 1. The formation energy diagrams using the SCAN functional for (a) F_C, (b) Cl_C, (c) Br_C, and (d) I_C.

31 July 2026 06:30:23

© Author(s) 2025

The charge transition levels (CTLs) of halogen substitutional defects in diamond are illustrated in Fig. 2. The CTLs represent the energies where a charge transition is taking place and they are directly computed by the crossing points of Fig. 1. These defects exhibit multiple charge states within the bandgap, confirming their electrically active nature and possible charge transitions. As reported before, the fluorine substitutional defect (F_C) exhibits CTLs at 0.64 eV [ε(+1/0)] and 3.10 eV [ε(0/−1)] above the valence band maximum (VBM), indicating a relatively deep donor–acceptor behavior. As we progress to heavier halogens, Cl, Br, and I, the transition levels shift higher within the bandgap. For instance, Cl_C has ε(+1/0) and ε(0/−1) located at 2.08 and 3.70 eV, respectively, while Br_C and I_C display transition levels at even higher energies, with I_C reaching up to 4.10 eV above the VBM.

These deep levels suggest that halogen defects in diamond are deep acceptors and donors. Their significant energetic distance from the VBM implies limited ionization at room temperature (295 K) and minimal contribution to free carrier concentrations under equilibrium conditions. Such behavior is typical of deep-level centers and aligns well with their potential use in quantum applications where charge state stability and optical activity are desired.

In Table I, we present the spin multiplicity of each defect. To find the correct spin multiplicity of the ground state of the defect, we examine the possible high- and low-spin configurations and we keep the ground state as the minimum energy. We predict that halogen doping provides a number of paramagnetic ground states, namely, in −1 charge, all defects exhibit a triplet ground state. As it was explained in methodology, the scope of this work is to identify the transition from the paramagnetic ground state to the paramagnetic excited state, meaning that for this work, singlet to singlet and doublet to doublet transitions are not examined. In Figs. 3(a)–3(l), we have collected the ground state of all halogen structures with respect to their bonding with the nearest C neighbors, while in Figs. 4(a)–4(d), the charge density of the halogen atoms and the nearest carbons are shown.

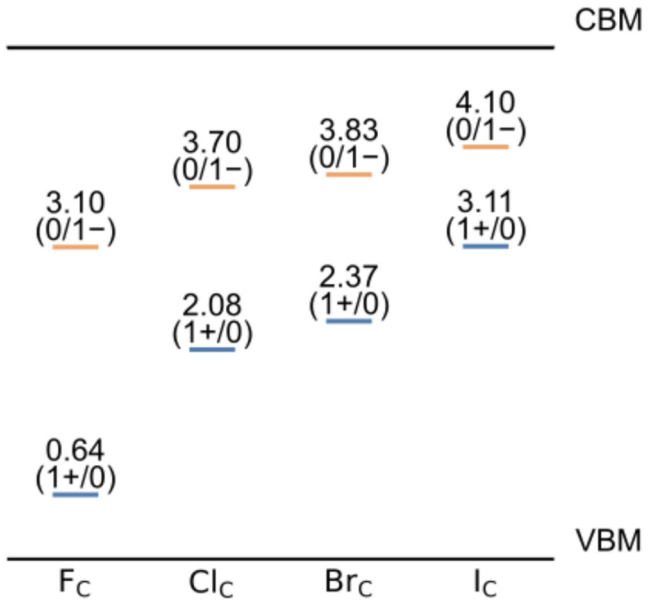

FIG. 2. The charge transition levels of all substitutional halogen impurities.

B. Electronic properties

After examining the thermodynamical stability and the spin state of the halogen defects in diamond, in this section, we discuss the electronic structure of those that could potentially be used as qubits. For the choice of the qubit defects, we follow the criteria of (a) paramagnetic ground state, (b) transition between occupied to unoccupied energy levels, and (c) stable low-spin state, which is located between the ground and excited states to provide an accessible intersystem crossing pathway. From our analysis, we found that the criteria for qubit spin defects are only met in the case of F_C^{-1}. The other halogens had either a diamagnetic ground state or they did not have available intersystem crossing pathways between the ground state and the excited state of the same spin configuration. Specifically, for all other defects, either they did not have two discrete states in the bandgap or states that could be accessed through intersystem crossing. For Fc^{-1}, we now investigate and present in Fig. 5(a) the electronic structure, through the Kohn–Sham energy levels at the gamma point, as they were computed directly from the ground state calculations. As it is seen, states are created by significant contributions from the p-orbital of fluorine. We observe distinct peaks within the bandgap which are well separated from one another. Notably, these features arise from the localized fluorine-derived states that hybridize with the carbon p-orbitals. The spin-up channel shows multiple occupied peaks created by the fluorine p-states.

In the spin-down channel, a single occupied state is present within the gap, while a degenerate state is unoccupied at higher energies. As the symmetry of the defect in the diamond host is C_{3v}, we used the respected group theory name for the states with "e," implying the degenerate state. The excitation at the spin-down channel resembles the NV^{-1} center a lot, with the degeneracy shifted close to the conduction band and is performed from the a_1 state to $e_{x,y}$.

As it was described by Weber *et al.*,[32,58] photoluminescence is the main optical property to manipulate the encoded qubit. One of the most important optical properties that describe the light–qubit interaction is the zero phonon line, which is sketched in Fig. 5(b), following the Franck–Condon approximation.[59,60] We calculate the

TABLE I. The defect energies and multiplicity of intrinsic defects for each charge state. Spin-multiplicity is presented as S for singlet, D for doublet, T for triplet, and Q for quartet.

Defect	Charge state			Spin multiplicity		
F_C	−1	0	+1	T	D	S
Cl_C	−1	0	+1	T	Q	T
Br_C	−1	0	+1	T	Q	S
I_C	−1	0	+1	T	D	S

31 July 2026 06:30:23

© Author(s) 2025

ZPL following the processes of Fig. 5(b) by using the Δ-SCF approach which is implemented in VASP and is proved to predict the energies in accordance to the experimental values.[44,61] Specifically, the curves include four states, A, B, C, and D. State A is the ground state of the system, while state B is the energy of the fixed ground state geometry when placing the spin-down a_1 electron to $e_{x,y}$. Geometry relaxation of the excited structure results in state C, and then fixing the relaxed geometry of state C and removing the excitation lead to state D. The energy difference of A–B and C–D are the absorption and emission, respectively. For the ZPL calculation, we used the SCAN functional which has shown excellent performance in the investigation of the N*V* center

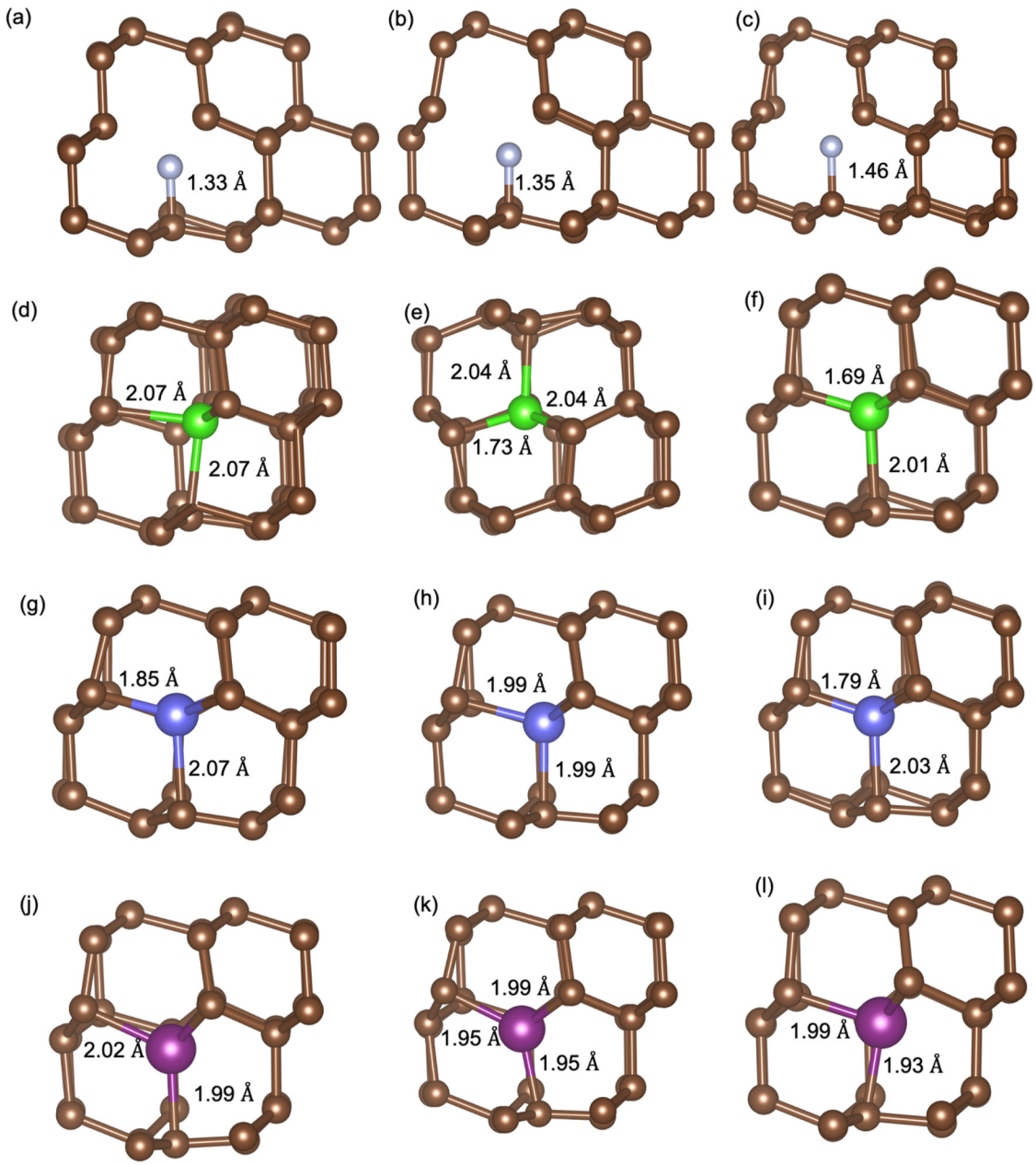

FIG. 3. The ground state geometry for (a) F_C^{-1}, (b) F_C^0, (c) F_C^{+1}, (d) Cl_C^{-1}, (e) Cl_C^0, (f) Cl_C^{+1}, (g) Br_C^{-1}, (h) Br_C^0, (i) Br_C^{+1}, (j) I_C^{-1}, (k) I_C^0, and (l) I_C^{+1}.

31 July 2026 06:30:23

© Author(s) 2025

and its related defects.[57] Our calculated ZPL is equal to 1.26 eV for the spin-down transition which is an attractive value for quantum applications. This value is much smaller compared to that of the NV center in diamond which is equal to 1.95 eV[62] but still is not in the telecommunication window. However, due to this low value, expect that fluorine doping in diamond can experience less optical loss during the transfer of the qubit to form a quantum network.

C. Spin qubit operation

We now explain the fluorine substitutional defect in diamond as a potential spin qubit. As shown in Fig. 6, this defect hosts a triplet ground state (^{3}A) and a triplet excited state (^{3}E) with an optical zero phonon line at 1.26 eV. We calculate the radiation lifetime for this transition to be 18.40 ns which is longer compared to the reported value for the NV center, which is 4.4 ns.[63] Furthermore, we compute the zero-field splitting of the spin-spin interaction between the $m_s = 0$ and $m_s = \pm 1$ sublevels in the triplet ground state at $|D| = 4.83$ GHz, placing it within an experimentally accessible regime for coherent spin manipulation. The quantum information is encoded at $m_s = 0$ and $m_s = \pm 1$ as $|0\rangle$ and $|1\rangle$ qubit states. The qubit initialization cycle follows a well described procedure.[34] Specifically, upon illumination, the system is excited to the triplet state from which it can decay non-radiatively through an intersystem crossing to a lower singlet state (^{1}E) and eventually repopulating the $|0\rangle$ sublevel of the ground state. This enables the spin initialization and readout via the spin-selective transition, similar to that of the NV^- center in diamond.

In Table II, we present the calculated hyperfine constants for F_C^{-1} in the triplet ground state. Our results reveal a localized defect

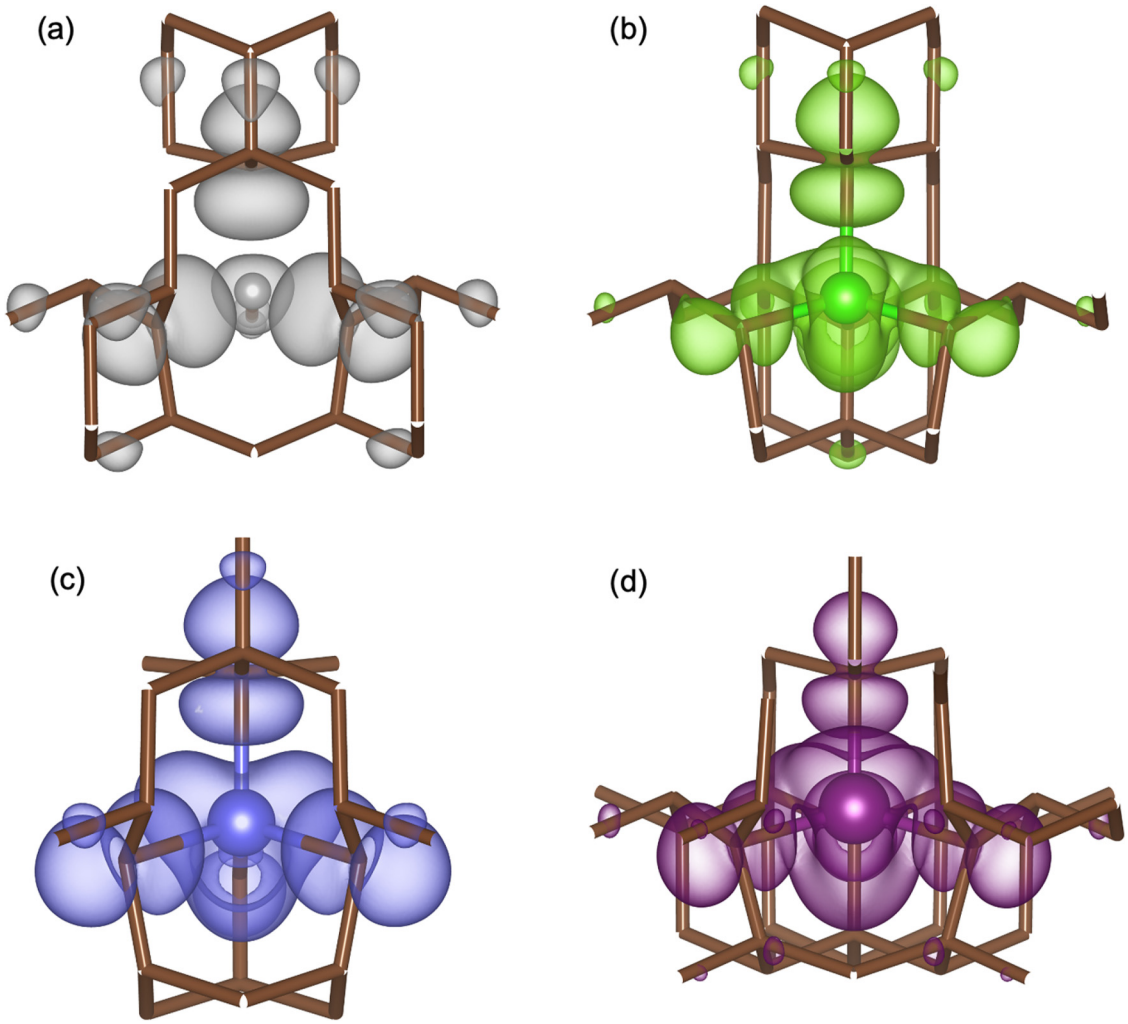

FIG. 4. The charge density for (a) F_C, (b) Cl_C, (c) Br_C, and (d) I_C.

31 July 2026 06:30:23

© Author(s) 2025

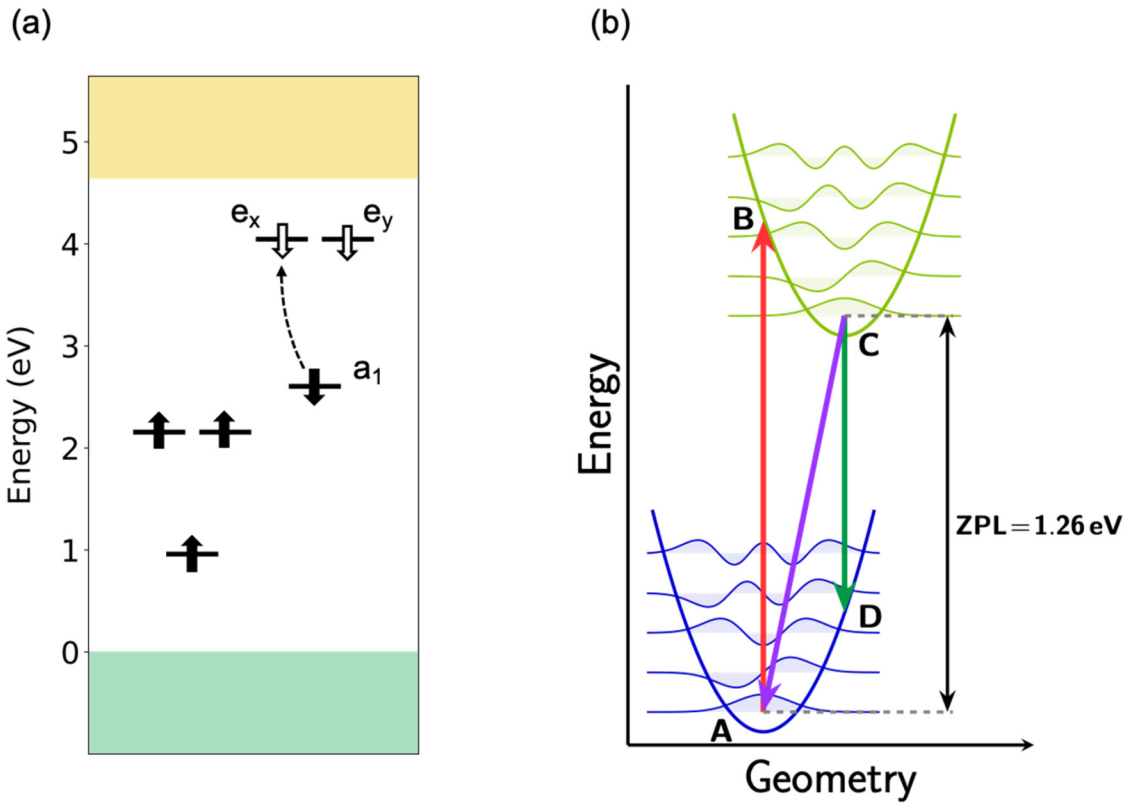

FIG. 5. (a) The Kohn–Sham levels at the gamma point for F_C^{-1} and (b) and the Franck–Condon principle used for the simulation of the excited state.

31 July 2026 06:30:23

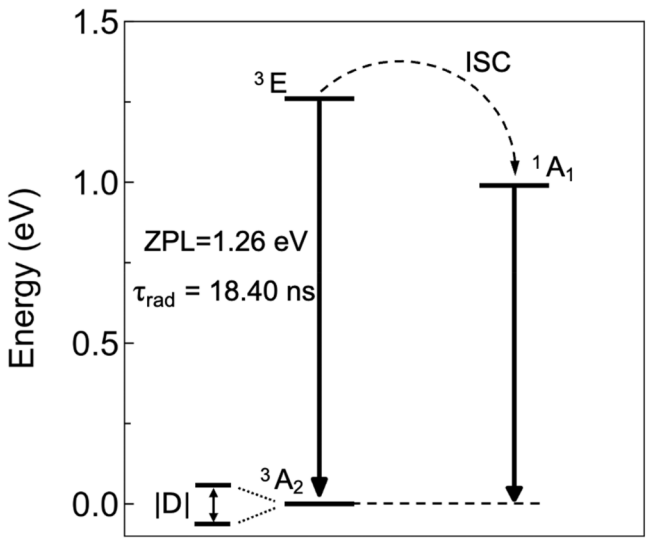

FIG. 6. Qubit operation for F_C^{-1} doped diamond.

which affects also the nearby C atoms. The large values of A_{xx} and A_{zz} show a large coupling to the ^{19}F nucleus at the defect site. The interaction with the neighbor ^{13}C shows much larger values. These interactions are very important for its performance as a qubit, specifically because coupling to nuclear spins is highly related to spin decoherence fluctuations and coherence time.[13] Moreover, the hyperfine interaction with nuclear spins can be a useful resource for quantum information processing (QIS), enabling the entanglement for applications in quantum memory and quantum error correction.

TABLE II. The calculated hyperfine constant with the SCAN functional with the contribution of the spin polarization of the core states (A_{1c}) in the Fermi-contact term. The table shows the data of F defects with the three nearest carbon neighbors.

	A_{xx}	A_{yy}	A_{zz}
^{19}F	32.65	−12.01	32.70
^{13}C	101.01	100.45	195.48
^{13}C	101.10	100.60	195.50
^{13}C	101.03	100.52	195.52

© Author(s) 2025

IV. CONCLUSIONS

In the present study, we employed the SCAN functional to investigate halogen doped diamond and its application in quantum technologies. We used the relatively new SCAN meta-GGA functional to evaluate thermodynamic stability, charge transition levels, electronic structure, and spin properties of the substitutional defects. Among these, the fluorine substitutional at negative charge was found as a particularly promising qubit candidate. Our calculations predicted that F_C^{-1} has a triplet ground state and optically addressable transitions with a ZPL at 1.26 eV. Moreover, its ZFS was calculated at 4.83 GHz. While its high formation energy is a limiting factor for synthesis, techniques such as ion implementation can be used to enable incorporation and stabilization. As a result, future experimental work is encouraged to verify the predicted properties and evaluate its feasibility for future quantum devices.

ACKNOWLEDGMENTS

We acknowledge support by computational time granted by the National Infrastructures for Research and Technology S.A. (GRNET S.A.) in the National HPC facility—ARIS—under Project ID pr017021. P.-P.F. would like to acknowledge Dr. Tom Irons from the University of Nottingham for the useful discussions.

AUTHOR DECLARATIONS

Conflict of Interest

The authors have no conflicts to disclose.

Author Contributions

Petros-Panagis Filippatos: Conceptualization (equal); Formal analysis (equal); Methodology (equal); Writing – original draft (equal); Writing – review & editing (equal). **Alexander Chroneos:** Resources (equal); Supervision (equal); Writing – original draft (equal); Writing – review & editing (equal). **Nikolaos Kelaidis:** Resources (equal); Software (equal); Writing – original draft (equal); Writing – review & editing (equal).

DATA AVAILABILITY

The data that support the findings of this study are available from the corresponding author upon reasonable request.

REFERENCES

[1]M. Atatüre, D. Englund, N. Vamivakas, S.-Y. Lee, and J. Wrachtrup, "Material platforms for spin-based photonic quantum technologies," Nat. Rev. Mater. **3**(5), 38–51 (2018).
[2]A. Acín, I. Bloch, H. Buhrman, T. Calarco, C. Eichler, J. Eisert, D. Esteve, N. Gisin, S. J. Glaser, F. Jelezko, S. Kuhr, M. Lewenstein, M. F. Riedel, P. O. Schmidt, R. Thew, A. Wallraff, I. Walmsley, and F. K. Wilhelm, "The quantum technologies roadmap: A European community view," New J. Phys. **20**(8), 080201 (2018).
[3]A. Chatterjee, P. Stevenson, S. De Franceschi, A. Morello, N. P. De Leon, and F. Kuemmeth, "Semiconductor qubits in practice," Nat. Rev. Phys. **3**(3), 157–177 (2021).
[4]M. Ruf, N. H. Wan, H. Choi, D. Englund, and R. Hanson, "Quantum networks based on color centers in diamond," J. Appl. Phys. **130**(7), 070901 (2021).
[5]S. Pezzagna and J. Meijer, "Quantum computer based on color centers in diamond," Appl. Phys. Rev. **8**(1), 011308 (2021).
[6]G. Wolfowicz, F. J. Heremans, C. P. Anderson, S. Kanai, H. Seo, A. Gali, G. Galli, and D. D. Awschalom, "Quantum guidelines for solid-state spin defects," Nat. Rev. Mater. **6**(10), 906–925 (2021).
[7]L. Childress, M. V. Gurudev Dutt, J. M. Taylor, A. S. Zibrov, F. Jelezko, J. Wrachtrup, P. R. Hemmer, and M. D. Lukin, "Coherent dynamics of coupled electron and nuclear spin qubits in diamond," Science **314**(5797), 281–285 (2006).
[8]M. W. Doherty, N. B. Manson, P. Delaney, F. Jelezko, J. Wrachtrup, and L. C. L. Hollenberg, "The nitrogen-vacancy colour centre in diamond," Phys. Rep. **528**(1), 1–45 (2013).
[9]Á. Gali, "*Ab initio* theory of the nitrogen-vacancy center in diamond," Nanophotonics **8**(11), 1907–1943 (2019).
[10]H. Bernien, B. Hensen, W. Pfaff, G. Koolstra, M. S. Blok, L. Robledo, T. H. Taminiau, M. Markham, D. J. Twitchen, L. Childress, and R. Hanson, "Heralded entanglement between solid-state qubits separated by three metres," Nature **497**(7447), 86–90 (2013).
[11]C. Zhang, F. Shagieva, M. Widmann, M. Kübler, V. Vorobyov, P. Kapitanova, E. Nenasheva, R. Corkill, O. Rhrle, K. Nakamura, H. Sumiya, S. Onoda, J. Isoya, and J. Wrachtrup, "Diamond magnetometry and gradiometry towards subpicotesla dc field measurement," Phys. Rev. Appl. **15**(6), 064075 (2021).
[12]I. Aharonovich and E. Neu, "Diamond nanophotonics," Adv. Opt. Mater. **2**(10), 911–928 (2014).
[13]H. Clevenson, M. E. Trusheim, C. Teale, T. Schröder, D. Braje, and D. Englund, "Broadband magnetometry and temperature sensing with a light-trapping diamond waveguide," Nat. Phys. **11**(5), 393–397 (2015).
[14]M. Toth and I. Aharonovich, "Single photon sources in atomically thin materials," Annu. Rev. Phys. Chem. **70**(1), 123–142 (2019).
[15]S. I. Azzam, K. Parto, and G. Moody, "Prospects and challenges of quantum emitters in 2D materials," Appl. Phys. Lett. **118**(24), 240502 (2021).
[16]S. Gupta, W. Wu, S. Huang, and B. I. Yakobson, "Single-photon emission from two-dimensional materials, to a brighter future," J. Phys. Chem. Lett. **14**(13), 3274–3284 (2023).
[17]G. Thiering and A. Gali, "Spin–orbit coupling and Jahn–Teller effect in T_d symmetry: An *ab initio* study on the substitutional nickel defect in diamond," Philos. Trans. R. Soc. A **382**(2265), 20220310 (2024).
[18]J. Davidsson, W. Stenlund, A. S. Parackal, R. Armiento, and I. A. Abrikosov, "Na in diamond: High spin defects revealed by the ADAQ high-throughput computational database," Npj Comput. Mater. **10**(1), 109 (2024).
[19]A. Chroneos, R. W. Grimes, and H. Bracht, "Fluorine codoping in germanium to suppress donor diffusion and deactivation," J. Appl. Phys. **106**(6), 063707 (2009).
[20]C. Monmeyran, I. F. Crowe, R. M. Gwilliam, C. Heidelberger, E. Napolitani, D. Pastor, H. H. Gandhi, E. Mazur, J. Michel, A. M. Agarwal, and L. C. Kimerling, "Improved retention of phosphorus donors in germanium using a non-amorphizing fluorine co-implantation technique," J. Appl. Phys. **123**(16), 161524 (2018).
[21]D. F. Downey, J. W. Chow, E. Ishida, and K. S. Jones, "Effect of fluorine on the diffusion of boron in ion implanted Si," Appl. Phys. Lett. **73**(9), 1263–1265 (1998).
[22]H. A. W. ElMubarek and P. Ashburn, "Reduction of boron diffusion in silicon–germanium by fluorine implantation," IEEE Electron Device Lett. **25**(8), 535–537 (2004).
[23]C. X. Yan, Y. Dai, and B. B. Huang, "DFT study of halogen impurity in diamond," J. Phys. Appl. Phys. **42**(14), 145407 (2009).
[24]S. F. Ahmed, D. Banerjee, and K. K. Chattopadhyay, "The influence of fluorine doping on the optical properties of diamond-like carbon thin films," Vacuum **84**(6), 837–842 (2010).
[25]A. K. Tiwari, J. P. Goss, P. R. Briddon, N. G. Wright, A. B. Horsfall, R. Jones, H. Pinto, and M. J. Rayson, "Calculated electron affinity and stability of halogen-terminated diamond," Phys. Rev. B **84**(24), 245305 (2011).
[26]K. J. Rietwyk, S. L. Wong, L. Cao, K. M. O'Donnell, L. Ley, A. T. S. Wee, and C. I. Pakes, "Work function and electron affinity of the fluorine-terminated (100) diamond surface," Appl. Phys. Lett. **102**(9), 091604 (2013).

31 July 2026 06:30:23

© Author(s) 2025

[27]D. Banerjee and K. K. Chattopadhyay, "Enhanced field emission properties of PECVD synthesized chlorine doped diamond like carbon thin films," Surf. Coat. Technol. **253**, 1–7 (2014).
[28]J. Zhou, C. Laube, W. Knolle, S. Naumov, A. Prager, F.-D. Kopinke, and B. Abel, "Efficient chlorine atom functionalization at nanodiamond surfaces by electron beam irradiation," Diam. Relat. Mater. **82**, 150–159 (2018).
[29]T. Lühmann, N. Raatz, R. John, M. Lesik, J. Rödiger, M. Portail, D. Wildanger, F. Kleißler, K. Nordlund, A. Zaitsev, J.-F. Roch, A. Tallaire, J. Meijer, and S. Pezzagna, "Screening and engineering of colour centres in diamond," J. Phys. Appl. Phys. **51**(48), 483002 (2018).
[30]T. Inoi, K. Baba, S. Flege, R. Hatada, and W. Ensinger, "Properties of iodine containing diamond-like carbon films prepared by plasma source ion implantation," Diam. Relat. Mater. **81**, 108–112 (2018).
[31]S. Ditalia Tchernij, T. Lühmann, E. Corte, F. Sardi, F. Picollo, P. Traina, M. Brajković, A. Crnjac, S. Pezzagna, Ž. Pastuović, I. P. Degiovanni, E. Moreva, P. Aprà, P. Olivero, Z. Siketić, J. Meijer, M. Genovese, and J. Forneris, "Fluorine-based color centers in diamond," Sci. Rep. **10**(1), 21537 (2020).
[32]J. R. Weber, W. F. Koehl, J. B. Varley, A. Janotti, B. B. Buckley, C. G. Van De Walle, and D. D. Awschalom, "Quantum computing with defects," Proc. Natl. Acad. Sci. U.S.A. **107**(19), 8513–8518 (2010).
[33]P. Udvarhelyi, B. Somogyi, G. Thiering, and A. Gali, "Identification of a telecom wavelength single photon emitter in silicon," Phys. Rev. Lett. **127**(19), 196402 (2021).
[34]S. Li, G. Thiering, P. Udvarhelyi, V. Ivády, and A. Gali, "Carbon defect qubit in two-dimensional WS_2," Nat. Commun. **13**(1), 1210 (2022).
[35]D. Dhaliah, Y. Xiong, A. Sipahigil, S. M. Griffin, and G. Hautier, "First-principles study of the T center in silicon," Phys. Rev. Mater. **6**(5), L053201 (2022).
[36]K. Jhuria, V. Ivanov, D. Polley, Y. Zhiyenbayev, W. Liu, A. Persaud, W. Redjem, W. Qarony, P. Parajuli, Q. Ji, A. J. Gonsalves, J. Bokor, L. Z. Tan, B. Kanté, and T. Schenkel, "Programmable quantum emitter formation in silicon," Nat. Commun. **15**(1), 4497 (2024).
[37]V. Ivády, I. A. Abrikosov, and A. Gali, "First principles calculation of spin-related quantities for point defect qubit research," Npj Comput. Mater. **4**(1), 76 (2018).
[38]R. Finsterhoelzl and G. Burkard, "Suppression of coherent errors during entangling operations in NV centers in diamond," arXiv:2503.17147 (2025).
[39]G. Kresse and J. Furthmüller, "Efficiency of *ab-initio* total energy calculations for metals and semiconductors using a plane-wave basis set," Comput. Mater. Sci. **6**(1), 15–50 (1996).
[40]G. Kresse and J. Furthmüller, "Efficient iterative schemes for *ab initio* total-energy calculations using a plane-wave basis set," Phys. Rev. B **54**(16), 11169–11186 (1996).
[41]G. Kresse and D. Joubert, "From ultrasoft pseudopotentials to the projector augmented-wave method," Phys. Rev. B **59**(3), 1758–1775 (1999).
[42]P. E. Blöchl, "Projector augmented-wave method," Phys. Rev. B **50**(24), 17953–17979 (1994).
[43]M. Maciaszek, V. Žalandauskas, R. Silkinis, A. Alkauskas, and L. Razinkovas, "The application of the SCAN density functional to color centers in diamond," J. Chem. Phys. **159**(8), 084708 (2023).
[44]G. Abbas, O. Bulancea-Lindvall, J. Davidsson, R. Armiento, and I. A. Abrikosov, "Theoretical characterization of NV-like defects in 4H-SiC using ADAQ with the SCAN and r2SCAN meta-GGA functionals," arXiv:2501.07289 (2025).
[45]C. Freysoldt, J. Neugebauer, and C. G. Van De Walle, "Fully *ab initio* finite-size corrections for charged-defect supercell calculations," Phys. Rev. Lett. **102**(1), 016402 (2009).
[46]S. R. Kavanagh, A. G. Squires, A. Nicolson, I. Mosquera-Lois, A. M. Ganose, B. Zhu, K. Brlec, A. Walsh, and D. O. Scanlon, "Doped: Python toolkit for robust and repeatable charged defect supercell calculations," J. Open Source Softw. **9**(96), 6433 (2024).
[47]V. Ivády, G. Barcza, G. Thiering, S. Li, H. Hamdi, J.-P. Chou, Ö. Legeza, and A. Gali, "*Ab initio* theory of the negatively charged boron vacancy qubit in hexagonal boron nitride," Npj Comput. Mater. **6**(1), 41 (2020).
[48]J. Davidsson, "Theoretical polarization of zero phonon lines in point defects," J. Phys.: Condens. Matter **32**(38), 385502 (2020).
[49]A. Alkauskas, C. E. Dreyer, J. L. Lyons, and C. G. Van De Walle, "Role of excited states in Shockley–Read–Hall recombination in wide-band-gap semiconductors," Phys. Rev. B **93**(20), 201304 (2016).
[50]M. J. Rayson and P. R. Briddon, "First principles method for the calculation of zero-field splitting tensors in periodic systems," Phys. Rev. B **77**(3), 035119 (2008).
[51]H. Xiang, C. Lee, H.-J. Koo, X. Gong, and M.-H. Whangbo, "Magnetic properties and energy-mapping analysis," Dalton Trans. **42**(4), 823–853 (2013).
[52]J. Li, L. Gu, and R. Wu, "Slow spin relaxation in single endohedral fullerene molecules," Phys. Rev. B **104**(22), 224431 (2021).
[53]H. L. Stern, Q. Gu, J. Jarman, S. E. Barker, N. Mendelson, D. Chugh, S. Schott, H. H. Tan, H. Sirringhaus, I. Aharonovich, and M. Atatüre, "Room-temperature optically detected magnetic resonance of single defects in hexagonal boron nitride," Nat. Commun. **13**(1), 618 (2022).
[54]K. Szász, T. Hornos, M. Marsman, and A. Gali, "Hyperfine coupling of point defects in semiconductors by hybrid density functional calculations: The role of core spin polarization," Phys. Rev. B **88**(7), 075202 (2013).
[55]R. Ren, X. Li, and J. Y. Yunwen, "The electronic transport characteristics in wide band-gap nitrogen vacancy diamond/Si hetero-structure using Raman spectrum," J. Cryst. Growth **532**, 125238 (2020).
[56]T. Hom, W. Kiszenik, and B. Post, "Accurate lattice constants from multiple reflection measurements. II. Lattice constants of germanium silicon, and diamond," J. Appl. Crystallogr. **8**(4), 457–458 (1975).
[57]D. Wang, L. Liu, and H. L. Zhuang, "Spin qubit based on the nitrogen-vacancy center analog in a diamond-like compound C_3BN," J. Appl. Phys. **130**(22), 225702 (2021).
[58]J. R. Weber, W. F. Koehl, J. B. Varley, A. Janotti, B. B. Buckley, C. G. Van De Walle, and D. D. Awschalom, "Defects in SiC for quantum computing," J. Appl. Phys. **109**(10), 102417 (2011).
[59]R. Ghassemizadeh, W. Körner, D. F. Urban, and C. Elsässer, "Stability and electronic structure of NV centers at dislocation cores in diamond," Phys. Rev. B **106**(17), 174111 (2022).
[60]J. Franck and E. G. Dymond, "Elementary processes of photochemical reactions," Trans. Faraday Soc. **21**, 536 (1926).
[61]P. H. Dederichs, S. Blügel, R. Zeller, and H. Akai, "Ground states of constrained systems: Application to cerium impurities," Phys. Rev. Lett. **53**(26), 2512–2515 (1984).
[62]G. Davies and M. F. Hamer, "Optical studies of the 1.945 eV vibronic band in diamond," Proc. R. Soc. London, Ser. A **348**(1653), 285–298 (1976).
[63]Y. Xiong, M. Mathew, S. M. Griffin, A. Sipahigil, and G. Hautier, "Midgap state requirements for optically active quantum defects," Mater. Quantum Technol. **4**(1), 013001 (2024).

31 July 2026 06:30:23

© Author(s) 2025